Structural Eng./Earthquake Eng., JSCE, Vol. 13, No. 2, 93s—104s, 1996 July
(J. Struct. Mech. Earthquake Eng., JSCE, No. 543/I—36)

# TIME DOMAIN MODELING OF BRIDGE DECK FLUTTER

K. WILDE[1], Y. FUJINO[2] and J. MASUKAWA[3]

[1] Member of JSCE, Ph.D., Assistant Professor,
Dept. of Civil Eng., University of Tokyo (Bunkyo-ku, Tokyo 113, Japan)
[2]Fellow Member of JSCE, Ph.D., Professor, Dept. of Civil Eng., University of Tokyo
[3]Member of JSCE, M. Eng., Research Institute of Kajima Corporation (Chofu-shi, Tokyo, Japan)

Time-domain modeling of bridge deck flutter is examined. The frequency dependent aerodynamic self-excited forces acting on a bridge deck are approximated in the Laplace domain by rational functions. Two matrix formulations of the rational function approximation, namely least-squares and minimum-state, are applied to aerodynamic data experimentally or theoretically obtained for various bridge decks. The precision of the approximations and the comparison of the critical wind speed computation by the conventional method and the proposed method are presented.

***Key Words :*** *bridge deck flutter, rational function approximation, multilevel optimization*

## 1. INTRODUCTION

The rapid development of technology made construction of bridges with the main span beyond 2000m possible. In design of very long bridges, wind induced phenomena become increasingly important; the critical condition is due to the flutter instability similar to one encountered in the aerospace structures. This paper is primarily devoted to derive a time-domain description of flutter of a bridge deck.

Flutter problem for airplane wings was solved by Theodorsen [1] in 1930s. The solution was derived from potential flow theory and describes the unsteady aerodynamic forces in terms of frequency dependent function. Roger [2] proposed the modeling method which can transform the aeroelastic equation of motion of an airplane into time domain. The method approximates aerodynamic force coefficients by rational functions of Laplace variable. The size of the equation after approximation is extended, but the overall analysis is greatly simplified.

The augmented system, in Roger's formulation, have relatively large number of added aerodynamic states and modifications of his method were proposed by Dunn [3] and Karpel [4] Further improvement of approximation performance was achieved by Tiffany et al. [5] by optimization of both linear and nonlinear coefficients of the approximating functions.

Most of constructed bridges have bluff girders and hence Theodorsen's approach results in significant modeling error. Scanlan [6] suggested a method which expresses self-excited aerodynamic forces with use of so-called *flutter derivatives* which can be determined for each type of a bridge deck by a specially designed wind tunnel experiment. The resulting equation of motion contains the flutter derivatives that are functions of reduced frequency, thus, the conventional analysis requires iterative search for a critical flutter wind speed. Moreover, material and geometrical nonlinearities in the structural system cannot be incorporated into the analysis and the dependence on reduced frequency limits the design of vibration suppression system to frequency domain methods.

Applicability of the rational modeling approach to the bridge flutter problem has not been examined in the field of bridge aerodynamics. This paper is

devoted to derive a state-space realization of the flutter equation of motion of a bridge deck.

The first part (Sec. 2) discusses the classical coupled flutter. The model for analytical analysis is simplified to the two-degree-of-freedom system. The unsteady aerodynamic forces for bluff (Sec. 2.1) and streamlined bridge deck cross-section (Sec. 2.2) are formulated and the governing equations of motion is derived. In Sec. 3 the concept of rational function approximation (RFA) is presented. The matrix formulations of RFA and resulting state-space equations are discussed in Sec. 4. Finally, the modeling method is applied to theoretically determined flutter derivatives and to experimentally obtained aerodynamic data of various bridge decks (Sec. 5).

## 2. EQUATION OF FLUTTER OF A BRIDGE DECK

Flutter is a self-excited oscillation. A structural system by means of its deflections and their time derivatives taps off energy from the wind flow. The critical flutter condition is the theoretical dividing line between the decaying and divergent self-excited motion with the certain speed of an oncoming smooth flow. The motion of the system subjected to an initial disturbance will either be damped or will grow indefinitely. The state of the system between the decaying and divergent motion, namely, sustained sinusoidal oscillation, is recognized as the critical flutter condition. The wind speed associated with the critical flutter condition will be referred to as *flutter wind speed.*

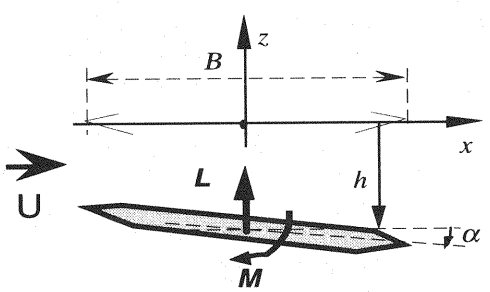


**Fig.1** 2DOF model of a bridge deck

A bridge deck (**Fig. 1**) is assumed to have two degrees-of-freedom: bending displacement, $h$, and torsional displacement, $\alpha$. The modes will be called *heaving* and *pitching,* respectively. The equation of motion is:

$$\begin{aligned} m\ddot{h} + c_h\dot{h} + k_h h &= -L \\ I_\alpha\ddot{\alpha} + c_\alpha\dot{\alpha} + k_\alpha\alpha &= M \end{aligned}, \qquad (1)$$

where a unit span of the system has mass $m$ and mass moment of inertia is $I_\alpha$, vertical and torsional restoring forces are characterized by spring constants $k_h$ and $k_\alpha$, and coefficients of viscous damping are $c_h$ and $c_\alpha$. Forces $L$ and $M$ represent the aerodynamic lift and moment about the rotation axis per unit span. The above equation describes a classical coupled bending-torsional flutter. Coupling between modes is due to the right-hand side of (1), i.e., unsteady aerodynamic forces. This coupling is the main reason for a very quick amplitude build up after the occurrence of the flutter condition, and it ultimately leads to total collapse of a bridge.

### (1) Aerodynamic Lift and Moment on a Bluff Bridge Deck

Flutter describes the complex structure-fluid interaction and practically in all cases involves non-linear aerodynamics. However, it has been possible to treat the problem successfully by linear analytical approaches, mainly because: the supporting structure is usually treatable as linearly elastic and its action dominates the form of the response, and because the flutter condition may be treated as having only small amplitudes.

The expressions for $L$ and $M$ for not "streamlined" bridge deck have not been possible to develop starting from basic fluid-flow principles. However, it has been shown by Scanlan [6] that for small oscillations the self-excited lift and moment on a bluff body may be treated as linear in the structural displacement and rotation and their first two derivatives, and that it is possible to measure the aerodynamic coefficients by means of wind tunnel tests. The aerodynamic coefficients are determined as functions of the reduced frequency $K$.

$$\begin{aligned} L &= \rho U^2 B\left\{KH_1^*\frac{\dot{h}}{U} + KH_2^*\frac{B\dot{\alpha}}{U} + K^2H_3^*\alpha + K^2H_4^*\frac{h}{B}\right\} \\ M &= \rho U^2 B^2\left\{KA_1^*\frac{\dot{h}}{U} + KA_2^*\frac{B\dot{\alpha}}{U} + K^2A_3^*\alpha + K^2A_4^*\frac{h}{B}\right\} \end{aligned}, \qquad (2)$$

where $\rho$ is air density, $U$ is the uniform approach velocity of the wind, $B$ is deck width, and reduced frequency $K$ is

$$K = \frac{B\omega}{U}. \qquad (3)$$

A circular frequency of oscillation is denoted by $\omega$. The coefficients $H_i^*$ and $A_i^*$ $(i=1,2,3,4)$ are non-dimensional functions of $K$. Inserting (2) into (1) and rewriting it in the matrix form yields

$$\mathbf{M}\ddot{\mathbf{q}}+\mathbf{C}\dot{\mathbf{q}}+\mathbf{K}\mathbf{q}=\frac{B}{U}\mathbf{V}_f\mathbf{Q}_1\dot{\mathbf{q}}+\mathbf{V}_f\mathbf{Q}_0\mathbf{q}, \tag{4}$$

where the vector of unknowns $\mathbf{q}$ is selected as

$$\mathbf{q}^t=\left[h/B \quad \alpha\right], \tag{5}$$

and is of size $n$. Coefficient matrices in (4) are defined as follows:

$$\mathbf{M}=\begin{bmatrix} mB & 0 \\ 0 & I_\alpha \end{bmatrix},\quad \mathbf{C}=\begin{bmatrix} 2\xi_h\omega_h mB & 0 \\ 0 & 2\xi_\alpha\omega_\alpha I_\alpha \end{bmatrix},$$

$$\mathbf{K}=\begin{bmatrix} \omega_h^2 mB & 0 \\ 0 & \omega_\alpha^2 I_\alpha \end{bmatrix},\quad \mathbf{V}_f=\begin{bmatrix} -0.5\rho U^2 B & 0 \\ 0 & 0.5\rho U^2 B^2 \end{bmatrix}$$

$$\mathbf{Q}_1=\begin{bmatrix} 2K_n^2H_4^* & 2K_n^2H_3^* \\ 2K_n^2A_4^* & 2K_n^2A_3^* \end{bmatrix},\quad \mathbf{Q}_0=\begin{bmatrix} 2K_nH_1^* & 2K_nH_2^* \\ 2K_nA_1^* & 2K_nA_2^* \end{bmatrix}. \tag{6}$$

Uncoupled natural frequencies of heaving and pitching mode are denoted by $\omega_h$ and $\omega_\alpha$, and damping ratios are $\xi_h$, $\xi_\alpha$, respectively. Since the flutter derivatives are obtained from the wind tunnel tests for specified values of the reduced frequency, they are not explicit functions of $K$. The coefficients of matrices $\mathbf{Q}_0$ and $\mathbf{Q}_1$ are determined for the selected set $\{K_n\}$, and are available in the form of tabular data.

### (2) Aerodynamic Lift and Moment on a Streamlined Bridge Deck

Aeroelastic behavior of a streamlined bridge deck may be assumed to be similar to a thin airfoil. The theoretical description of unsteady aerodynamic forces on an elasticity supported thin plate was derived by Theodorsen [1]. The expressions for $L$ and $M$ are linear in $h$ and $\alpha$, and their first and second derivatives, i.e.,

$$L=\pi\rho b^2\left\{\ddot{h}+U\dot{\alpha}\right\}+2\pi\rho UbC(k)\left\{\dot{h}+U\alpha+\frac{b}{2}\dot{\alpha}\right\}$$

$$M=\pi\rho b^3\left\{-\frac{U}{2}\dot{\alpha}-\frac{b}{8}\ddot{\alpha}\right\}+\pi\rho Ub^2C(k)\left\{\dot{h}+U\alpha+\frac{b}{2}\dot{\alpha}\right\} \tag{7}$$

where $b$ is the half-chord of the airfoil and $C(k)$ is the complex function known as *Theodorsen's circulatory function*. The terms in $\ddot{h}$ and $\ddot{\alpha}$ in equation (7) are important in aeronautical applications, but in wind aerodynamic problems they are negligible, and are therefore omitted. Then, equation (7) can be transformed into the form of (2). The coefficients $H_i^*$ and $A_i^*$ $(i=1,2,3,4)$ are now determined analytically and are found to be:

$$\begin{aligned} H_1^* &= \frac{1}{4}\cdot\frac{2\pi F}{k},\quad H_2^*=\frac{1}{8}\frac{\pi}{k}\left(1+F+\frac{2G}{k}\right), \\ H_3^* &= \frac{1}{8}\cdot\frac{2\pi}{k^2}\left(F-\frac{kG}{2}\right),\quad H_4^*=-\frac{1}{4}\cdot\frac{2\pi G}{k}, \\ A_1^* &= \frac{1}{8}\cdot\frac{\pi F}{k},\quad A_2^*=\frac{1}{16}\cdot\frac{\pi}{2k}\left(-1+F+\frac{2G}{k}\right), \\ A_3^* &= \frac{1}{16}\frac{\pi}{k^2}\left(F-\frac{kG}{2}\right),\quad A_4^*=-\frac{1}{8}\frac{\pi G}{k}, \end{aligned} \tag{8}$$

where $k=B\omega/(2U)$. $F$ and $G$ denote the real and imaginary parts of Theodorsen's function,

$$C(k)=F(k)+iG(k)=\frac{H_1^2(k)}{H_1^2(k)+H_0^2(k)}. \tag{9}$$

$H_n^2(k)$ is a combination of Bessel functions of the first $J_n$ and second $Y_n$ kinds,

$$H_n^2(k)=J_n-iY_n,\quad n=0,1. \tag{10}$$

The equation of motion of a flexible bridge with the aerodynamic forces determined by Theodorsen's approach can be written in the form of equation (4).

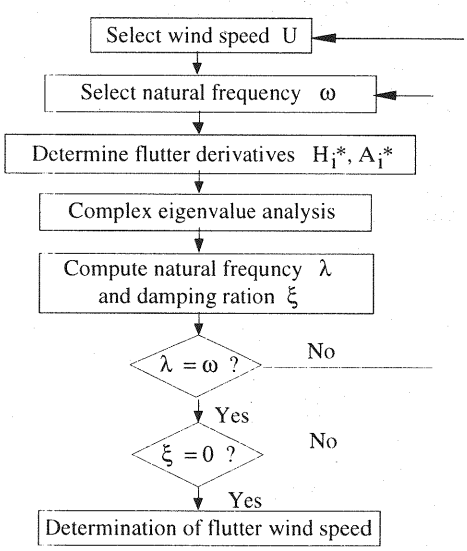


**Fig.2** Algorithm for computation of critical flutter wind speed

**(3) Solution for flutter critical wind speed**

Since the equation of motion of flutter (1) has the frequency dependent components in the terms describing unsteady aerodynamic forces (2), the solution for the critical flutter wind speed has to be done in an iterative way. The algorithm for conventional determination of critical flutter wind speed is presented in **Fig. 2.**

## 3. RATIONAL FUNCTION APPROXIMATION TO UNSTEADY AERODYNAMIC FORCES

The notation of the flutter equation (4) can be further simplified by combining matrices $\mathbf{Q}_0$ and $\mathbf{Q}_1$ into the complex form,

$$\mathbf{Q} = \begin{bmatrix} 2K_n{}^2 H_4^* + i2K_n{}^2 H_1^* & 2K_n{}^2 H_3^* + i2K_n{}^2 H_2^* \\ 2K_n{}^2 A_4^* + i2K_n{}^2 A_1^* & 2K_n{}^2 A_3^* + i2K_n{}^2 A_2^* \end{bmatrix}. \tag{11}$$

Thus, the equation of motion becomes

$$\mathbf{M}\ddot{\mathbf{q}} + \mathbf{C}\dot{\mathbf{q}} + \mathbf{K}\mathbf{q} = \mathbf{V}_f \mathbf{Q}\mathbf{q} \ . \tag{12}$$

The tabular data which describe the unsteady aerodynamics is now represented by matrix $\mathbf{Q}$.

Taking Laplace transforms in equation (12) with assumption of zero initial conditions gives

$$\left(\mathbf{M}s^2 + \mathbf{C}s + \mathbf{K}\right) \mathrm{L}(\mathbf{q}) = \mathbf{V}_f \mathbf{Q}\, \mathrm{L}(\mathbf{q}) \ , \tag{13}$$

where $L$ denotes Laplace operator.

Approximation of unsteady aerodynamic forces as rational functions of Laplace variable allows the aeroelastic equation of motion to be cast in a linear time invariant state-space realization. The most common form of the approximating functions used currently in aeronautics for each generalized force coefficient $\mathbf{Q}_{ij}$ of $\mathbf{Q}$ is a rational function of the nondimensional Laplace variable $p$:

$$\hat{\mathbf{Q}}_{ij}(p) = \left(\mathbf{A}_0\right)_{ij} + \left(\mathbf{A}_1\right)_{ij} p + \sum_{\ell=1}^{n_\ell} \left(\mathbf{A}_{\ell+1}\right)_{ij} \frac{1}{p+\lambda_\ell}, \tag{14}$$

where the hat over $\mathbf{Q}_{ij}$ denotes approximation and

$$p = \frac{B}{U} s = iK \tag{15}$$

The partial fractions, $\mathbf{A}_{\ell+1}/(p+\lambda_\ell)$, are commonly called *lag terms*, because each represents a transfer function in which the output "lags" the input and permits an approximation of the time delays inherent in unsteady aerodynamics. The coefficients of the partial fractions $\lambda_\ell$ are referred as *lag coefficients*. Addition of each partial fraction results in introducing into the state-space realization, obtained through rational modeling, new states, referred as *aerodynamic states*. The number of partial fractions is denoted by $n_\ell$ and this number is found as a compromise between the precision of the approximation and the size of aerodynamic dimension. *Aerodynamic dimension* is defined as a number of newly added aerodynamic states.

In view of (15) the approximation is performed only for oscillatory motion since $p$ is purely imaginary. In order to obtain solutions on the Laplace domain for both growing and decaying motion it is necessary to express the forces as a function of $s$ for the entire complex $s$-plane, or equivalently for the nondimensionalized complex $p$-plane. To overcome this, the concept of analytic continuation is often used [5], which justifies extending these functions, to the entire complex plane by finding analytic functions which agree with the aerodynamic forcing functions at all values of frequencies. However, there are only a finite number of frequencies at which tabular data are available; hence, this process is at best an approximate analytic continuation into the region near the portion of the axis containing the tabular data. Since flutter phenomena occurs for points in the complex $s$-plane which lie along the $i\omega$-axis, approximations into the region near the axis are sufficient for most studies.

Formula (14) assumes approximation of each element of $\mathbf{Q}$ independently, and therefore imposes separate selection of the lag coefficients for each $\mathbf{Q}_{ij}$. However, such approach results in unnecessary big state-space realizations and significantly increases computational burdens. More convenient handling of approximation can be obtained by application of selected matrix formulations of RFA's.

## 4. MATRIX FORMULATIONS OF RATIONAL FUNCTION APPROXIMATION

There are several variations of the matrix form of the rational function approximations (RFA's) for the unsteady aerodynamic force coefficients. Two of them, namely the least-squares and minimum state formulation, are considered. Each matrix formulation results in different aerodynamic state vectors.

**(1) Least-Squares (LS) RFA Formulation**

Roger [2] and, later Abel [7], formulated the rational function approximation so as to use the same denominator coefficients $\lambda_\ell$ for all the elements $\mathbf{Q}_{ij}$. of the matrix $\mathbf{Q}$ in order to reduce the number of aerodynamic states resulting in state-space. The above condition allows the "per element" expressions of (14) to be valid for the whole matrix $\mathbf{Q}$:

$$\hat{\mathbf{Q}}(p) = \mathbf{A}_0 + \mathbf{A}_1 p + \sum_{\ell=1}^{n_\ell} \mathbf{A}_{\ell+1} \frac{1}{p+\lambda_\ell} \qquad (16)$$

Each matrix in (16) is square, with dimensions $n \times n$ ($n$ is the dimension of the vector of unknowns). To derive state-space representation, equation (16) is inserted into Laplace domain equation of motion (13) i.e.,

$$\left(\mathbf{M}s^2 + \mathbf{C}s + \mathbf{K}\right) L(\mathbf{q}) = \mathbf{V_f}\left(\mathbf{A}_0 + \mathbf{A}_1 p + \sum_{\ell=1}^{n_\ell} \mathbf{A}_{\ell+1} \frac{1}{p+\lambda_\ell}\right) L(\mathbf{q}) \qquad (17)$$

If the aerodynamic states are defined by

$$L(\mathbf{xa}_\ell) = \frac{1}{p+\lambda_\ell} L(\mathbf{q}), \qquad (18)$$

the Laplace domain equations becomes

$$\left(\mathbf{M}s^2 + \mathbf{C}s + \mathbf{K}\right) L(\mathbf{q}) = \mathbf{V_f}\left(\mathbf{A}_0 L(\mathbf{q}) + \mathbf{A}_1 p\, L(\mathbf{q}) + \sum_{\ell=1}^{n_\ell} \mathbf{A}_{\ell+1} L(\mathbf{xa}_\ell)\right) \qquad (19a,b)$$

$$L(\mathbf{xa}_\ell) p + L(\mathbf{xa}_\ell)\lambda_\ell = L(\mathbf{q})$$

Thus, taking the inverse Laplace transforms in (19) gives time domain equations of the form:

$$\mathbf{M}\ddot{\mathbf{q}} + \mathbf{C}\dot{\mathbf{q}} + \mathbf{K}\mathbf{q} = \mathbf{V_f}\,\mathbf{A}_0\,\mathbf{q} + \frac{B}{U}\mathbf{V_f}\,\mathbf{A}_1\,\dot{\mathbf{q}} + \mathbf{V_f}\sum_{\ell=1}^{n_\ell} \mathbf{A}_{\ell+1}\ \mathbf{xa}_\ell \qquad (20a,b)$$

$$\frac{B}{U}\dot{\mathbf{xa}}_\ell + \lambda_\ell \mathbf{xa}_\ell = \mathbf{q}$$

Equation (20) is not dependent on reduced frequency $K$ and represents a linear time invariant system. The second equation, i.e. equation (20b) gives the mathematical description of newly introduced aerodynamic states. They are governed by first order differential equations with vertical and torsional displacements considered as inputs. Each aerodynamic vector $\mathbf{xa}_\ell$ is of the same size as vector $\mathbf{q}$. The aerodynamic states can be looked as states which model the air behavior of the incoming flow around the bridge deck.

A state-space realization of equation (20) can be selected as:

$$\begin{bmatrix} \ddot{\mathbf{q}} \\ \dot{\mathbf{q}} \\ \dot{\mathbf{xa}}_1 \\ \vdots \\ \dot{\mathbf{xa}}_{n_\ell} \end{bmatrix} = \begin{bmatrix} -\mathbf{M}^{-1}\mathbf{C}_t & -\mathbf{M}^{-1}\mathbf{K}_t & \mathbf{M}^{-1}\mathbf{V}_f\mathbf{I} & \cdots & \mathbf{M}^{-1}\mathbf{V}_f\mathbf{I} \\ \mathbf{I} & \mathbf{0} & \mathbf{0} & \cdots & \mathbf{0} \\ \mathbf{0} & U/B \cdot \mathbf{A}_2 & -U/B \cdot \lambda_1\mathbf{I} & \cdots & \mathbf{0} \\ \vdots & \vdots & \vdots & \ddots & \vdots \\ \mathbf{0} & U/B \cdot \mathbf{A}_{n_\ell+1} & \mathbf{0} & \cdots & -U/B \cdot \lambda_{n_\ell}\mathbf{I} \end{bmatrix} \begin{bmatrix} \dot{\mathbf{q}} \\ \mathbf{q} \\ \mathbf{xa}_1 \\ \vdots \\ \mathbf{xa}_{n_\ell} \end{bmatrix} \qquad (21)$$

were $\mathbf{C}_t = \mathbf{C} - (B/U)\mathbf{V}_f\mathbf{A}_0$ and $\mathbf{K}_t = \mathbf{K} - \mathbf{V}_f\mathbf{A}_1$ are the bridge deck total damping and stiffness, respectively. Since $\mathbf{A}_{\ell+1}$ is of the size $n$, there are exactly $n$ states for each $\ell = 1, \ldots, n_\ell$. This implies that the number of added aerodynamic states (aerodynamic dimension) for state-space realization of the least-squares RFA formulation is

$$n_a = n \cdot n_\ell \,. \qquad (22)$$

**(2) Minimum State (MS) RFA Formulation**

In reference [4], Karpel suggested a method in order to find a minimal augmented state vector, the process of finding aerodynamic approximations and the determining the state-space equations should be reversed.

The derivation starts with the general form of the state-space equation defined by

$$\begin{bmatrix} \ddot{\mathbf{q}} \\ \dot{\mathbf{q}} \\ \dot{\mathbf{xa}} \end{bmatrix} = \begin{bmatrix} -\mathbf{M}^{-1}\left[\mathbf{C} - (B/U)\mathbf{V}_f\mathbf{A}_0\right] & -\mathbf{M}^{-1}\left[\mathbf{K} - \mathbf{V}_f\mathbf{A}_1\right] & \mathbf{M}^{-1}\mathbf{V}_f\mathbf{D} \\ \mathbf{I} & \mathbf{0} & \mathbf{0} \\ \mathbf{0} & (U/B)\mathbf{E} & (U/B)\mathbf{R} \end{bmatrix} \begin{bmatrix} \dot{\mathbf{q}} \\ \mathbf{q} \\ \mathbf{xa} \end{bmatrix} \qquad (23)$$

where $\mathbf{D}$ and $\mathbf{E}$ are rectangular matrices of size $n \times n_\ell$ and $n_\ell \times n$ respectively, and $\mathbf{R}$ is a diagonal matrix of the form

$$\mathbf{R} = \begin{bmatrix} \lambda_1 & \cdots & 0 \\ \vdots & \ddots & \\ 0 & & \lambda_{n_\ell} \end{bmatrix}. \qquad (24)$$

Thus, the aerodynamic approximations which satisfies equations (23) and (24) results in the formula

$$\hat{\mathbf{Q}}(p) = \mathbf{A}_0 + \mathbf{A}_1 p + \mathbf{D}(p\mathbf{I} - \mathbf{R})^{-1}\mathbf{E} \,. \qquad (25)$$

Rewriting Eq. (25) for a single element of $\mathbf{Q}$ gives:

$$\hat{\mathbf{Q}}(p)_{ij} = (\mathbf{A}_0)_{ij} + (\mathbf{A}_1)_{ij}\, p + \sum_{\ell=1}^{n_\ell} D_{i\ell}\, E_{\ell j}\, \frac{1}{p+\lambda_\ell} \,. \quad (26)$$

Since $\mathbf{R}$ is of dimension $n_\ell \times n_\ell$ the aerodynamic dimension for the minimum-state RFA formulation is:

$$n_a = n_\ell \,. \quad (27)$$

For each additional lag term the size of the resulting state-space realization is bigger only by one aerodynamic state. Thus, introduction of lager number of lag terms does not increase the state-space realization significantly.

**(3) Multilevel Optimization: Linear and Nonlinear**

Minimization of approximation errors can be achieved by increasing the number of lag term, but as shown in previous sections, it adversely increases the number of equations required to define the aerodynamic system. Improvement can also be obtained by reducing the frequency range over which the fits are required, but this narrows the applicability of the approximation. The additional improvements may be gained by an optimization of the lag coefficients.

From (14) it is clearly seen that the coefficients $(\mathbf{A}_0)_{ij}$, $(\mathbf{A}_1)_{ij}$ and $(\mathbf{A}_{\ell+1})_{ij}$ may be found through a linear optimization, e.g., in the least-squares sense, but the lag coefficients must be searched via a nonlinear optimization method. Determination of parameters of approximation functions (16) and (25) is divided into two parts: optimization of coefficients $(\mathbf{A}_m)_{ij}$ $(i,j=1,\ldots,n;\ m=0,\ldots,n_\ell+1)$ and search for $\lambda_\ell$. Each process requires a multilevel optimization in the sense that closed form linear least-squares solution for linear parameters is performed inside an iterative search for parameters that enter the problem in a nonlinear fashion. In edition, each method requires that the characteristic roots of the system matrix corresponding to the aerodynamic states are stable.

**a) Linear optimization**

To determine the linear parameters in the RFA's, a measure of error between the approximating curve and the actual tabular data for each aerodynamic force element is defined by

$$\varepsilon_{ij} = \frac{\sum_n \left\| \hat{\mathbf{Q}}_{ij}(iK_n) - \mathbf{Q}_{ij}(iK_n) \right\|^2}{M_{ij}}, \quad (28)$$

where

$$M_{ij} = \max_n \left\{ 1, \left\| \mathbf{Q}_{ij}(iK_n) \right\|^2 \right\},$$

and $\{K_n\}$ is a set of reduced frequencies for which tabular data are available.

Each term in the sum in (28) is a measure of relative error, if the maximum magnitude of $\mathbf{Q}_{ij}(iK_n)$ is greater then 1, but is an absolute error for magnitudes less then 1. This error function essentially normalizes the aerodynamic data prior to the nonlinear optimization.

Since the coefficients $(\mathbf{A}_m)_{ij}$ are used as design variables and (28) satisfies the minimum condition, all partial derivatives with respect to each design variable must be 0, that is,

$$\frac{\partial \varepsilon_{ij}}{\partial (A_m)_{ij}} = 0 \quad (for \quad m = 0,\cdots,n_\ell+1) \quad (29)$$

Then, the resulting system of equations is linear. Linear algebraic methods may be employed to determine the exact optimal solution.

**b) Nonlinear optimization**

The technique employed herein to optimize $\lambda_\ell$ is a nongradient method developed by Nelder and Mead. In this application the nongradient optimizer has been found to be numerically stable and to possess good convergence properties. The nonlinear parameters are selected so as to reduce the total approximation error,

$$J = \sqrt{\sum_j \sum_i w_{ij}\, \varepsilon_{ij}} \,. \quad (30)$$

The weighting factors are used to force some of the elements to have more priority than others in determining the lag coefficients.

**c) Side constrains for nonlinear optimization**

Since the newly introduced states are governed by first order differential equations with lags terms as a coefficients (20), they must be bigger than 0, in order to ensure system stability. Also, it is desired to restrict the range of variation to that in the neighborhood of the range of frequencies over which tabular data are available, e.g.,

$$0 \le L_\ell \le \lambda_\ell \le U_\ell \qquad (for \quad \ell = 1,\ldots,n_\ell), \quad (31)$$

where $L_\ell$ and $U_\ell$ denote, respectively, lower and upper limit imposed on $\ell$-th lag coefficient. These side constraints are enforced by an inverse sinusoidal transformation of the design space

$[L_\ell, U_\ell]$ onto the real line segment [-1,+1]. The relationship between them is:

$$\lambda_\ell = \frac{U_\ell - L_\ell}{2}\sin(\frac{\pi}{2}z_\ell) + \frac{U_\ell + L_\ell}{2}, \qquad (32)$$

where

$$-1 \le z_\ell \le 1.$$

This transformation ensures that the side constraints are always satisfied.

## 5. APPLICATION OF RATIONAL FUNCTION APPROXIMATIONS

The unsteady aerodynamic forces of various bridge girders were approximated by the least-squares and minimum-state RFA formulation. Approximations were conducted for the number of lag terms from 1 to 6. In both formulations the weighting factors in the total approximation error (30) were chosen to be 1.0, and the fits were done over the entire frequency range for all elements. The approximations were performed through linear and nonlinear constrained optimization.

The following results are presented only for the number of lags equal to 1, 2 and 3, since it was found that for all the cases such size of the approximation function provides sufficient precision of the fit. The increase of lags beyond 3 reduces the approximation error, however, the computation burden is considerably increased. Especially, the nonlinear optimization of lags becomes troublesome since it requires careful selection of its initial values.

The aim of this simulations is to determine the necessary size of the approximating functions for given cross sections and to evaluate a more convenient RFA formulation.

### (1) Approximations of Aerodynamic Forces of Various Bridge Decks

The approximations were performed on the aerodynamic data, obtained form experiment, of the following types of girders: flat box, bluff box, conventional truss, truss with vertical stabilizer and central barrier, flat and bluff rectangular cross section. The RFA's were also applied to theoretically determined flutter derivatives of streamlined girder. The complete results of the approximations are presented in reference [8].

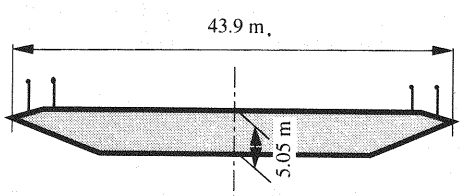


**Fig.3** Flat box cross-section proposed for Akashi Bridge

**a) Flat and bluff box girder**

The geometry of a flat box cross-section is shown in **Fig. 3**. A bluff box had the analogical shape with depth of 8.07m. Both cross sections were proposed for Akashi Kaikyo Bridge and tested in wind tunnel. The unsteady aerodynamic data is presented by Fujino, Iwamoto, et al. in [9]. The flutter derivatives were determined for wind angle of attack 0 and 5 degree for the flat box girder, and 0, 3 degree for the bluff box section. The sets of reduced frequencies was selected as $\{K_n\}$ = {0.360, 0.389, 0.428, 0.469, 0.522, 0.590, 0.681, 0.791, 0.960} for the flutter

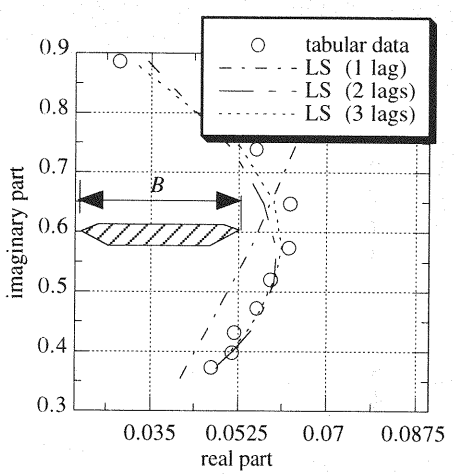


a) Least-squares RFA formulation

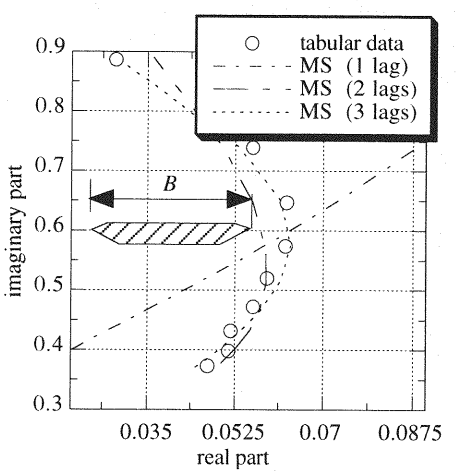


a) Minimum state RFA formulation

**Fig.4** Approximation of pitching moment due to heaving mode, $Q_{21}$, of flat box girder with different number of lag terms

derivatives associated with heaving mode, and $\{K_n\}$ = {0.36, 0.39, 0.427, 0.470, 0.523, 0.589, 0.676, 0.797, 0.966} for the flutter derivatives associated with pitching mode. Some of the results of the approximations by least-squares (LS) RFA formulation and the minimum-state (MS) method are shown in **Fig. 4**. For this girder approximation of pitching moment due to heaving mode was the most difficult.

Approximation by the least squares and minimum state RFA formulation gives similar results with respect to the number of lag terms in the approximation functions. It was found that satisfactory approximation precision is obtained by using two lag coefficients.

**b) Truss girder**

The flutter derivatives of a conventional truss cross section (**Fig. 5**) and its modification with vertical stabilizer and center barrier, selected for Akashi Kaikyo Bridge, were obtained by Honshu

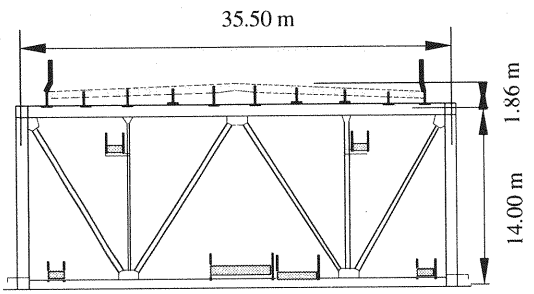


**Fig.5** Truss cross-section proposed for Akashi Bridge [10)]

Shikoku Bridge Authority [10)]. The flutter derivatives were determined for both sections for the wind angle of attack 0 and 3 degrees.

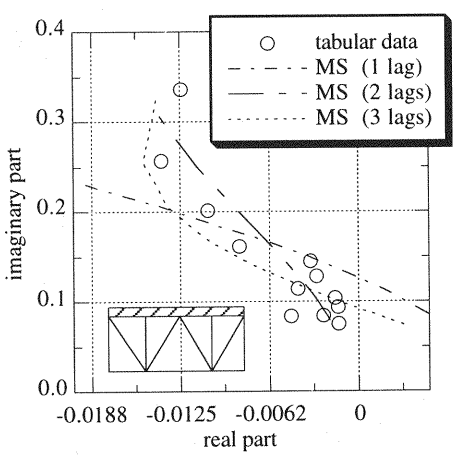


a) For wind angle of attack 0 degree

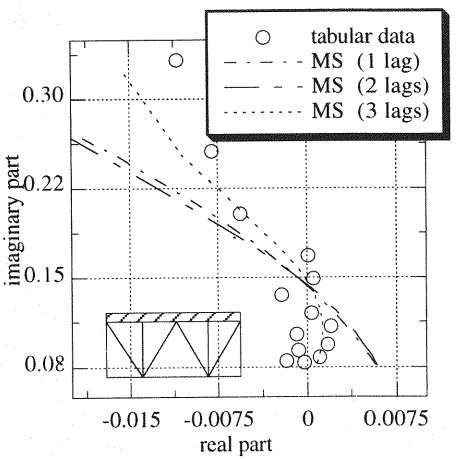


b) For wind angle of attack 3 degree

**Fig.6** Approximation of pitching moment due to heaving mode, $\mathbf{Q}_{21}$, of the truss girder by MS RFA

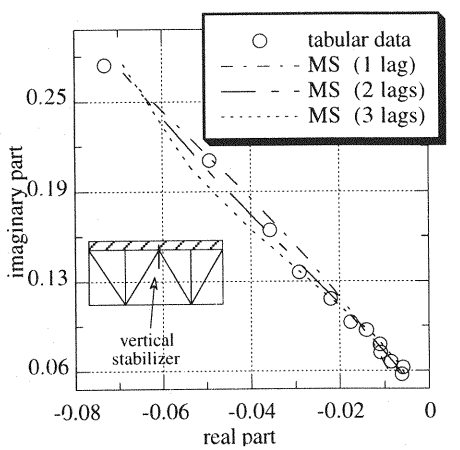


a) Approximation of pitching moment due to heaving, $\mathbf{Q}_{21}$

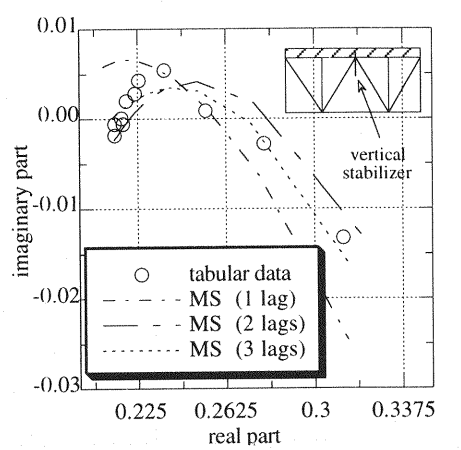


b) Approximation of pitching moment due to pitching, $\mathbf{Q}_{22}$

**Fig.7** Approximation of the truss girder with vertical stabilizer by MS RFA

The approximation of pitching moment due to heaving mode for the case of conventional truss girder (**Fig. 6a**) was the most difficult component of the aerodynamic force to approximate. The approximation error of this section with angle of attack 3 degree (**Fig. 6b**) was found to be larger.

The addition of vertical stabilizer and central barrier in the truss section significantly changes the distribution of the flutter derivatives data. The most difficult component of the forces, in this case, was found to be pitching moment due to pitching mode (**Fig. 7b**), while pitching moment due to heaving mode (**Fig. 7a**) could be easily approximated with one lag coefficient.

**Figures 6** and **7** show differences in the agreement between the experimental data and the approximations. Since the approximating function consists of linear part, $a_o+a_1p$ ($a_o, a_1$ - real values), and a set of hyperbolic function, $a_{l+}/(p+\lambda_\ell)$ ($a_{l+}$, $\lambda_\ell$- real values), it can easily perform the approximation if data are distributed along line, like in **Fig. 7a**, or along the curve with a curvature of a constant sign (**Fig. 4**). If the data is such that it should be represented by a curve with inflection point, it is necessary to increase the number of lag terms in the approximation function. The linear coefficients of the approximation function, $\mathbf{A}_i$ ($i$ =1,2,...), are determined by least squares optimization, thus, concentration of experimental points in one region (e.g., **Fig. 6**) causes that the approximation provides poor fit in the other regions. The approximation given in **Fig. 6** and **7b** could be improved by limiting the data for RFA's in the region where the data are concentrated or by introducing weightings which would increase the importance of the regions with small number of experimental points.

In general, the approximation of conventional truss section and truss with vertical stabilizer can be sufficiently represented by RFA's with three lag coefficients in the approximation functions. There are no significant difference in the approximation error of the least squares and minimum states RFA formulation with respect to a number of lag coefficients.

**c) Rectangular cross section**

Rectangular cross sections with the ratios of width to depth 5 and 8 were experimentally tested by Matsumoto et al. [11]. The rational approximations of pitching moment due to heaving mode by the minimum state RFA formulation are presented in **Fig. 8**. For the section with the ratio 5 the satisfactory precision of the fit was achieved by using two or three lag terms in the approximating functions. However, the approximation of the aerodynamic forces of the section with ratio 8 (**Fig. 8b**) was difficult to obtain due to scattered character of data and limited amount of points.

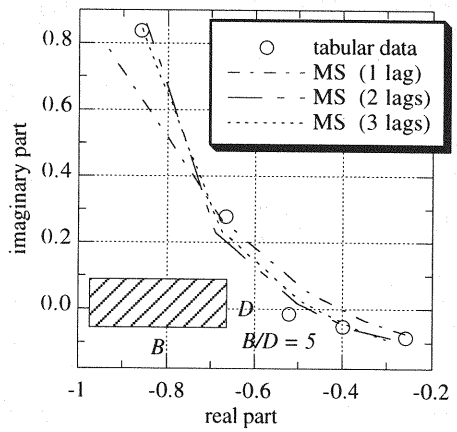


a) Cross section with the ratio of 5

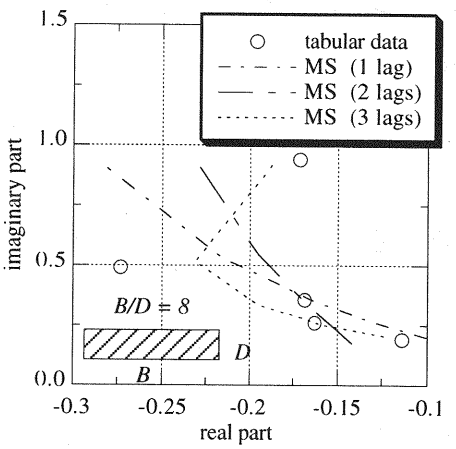


b) Cross section with the ratio of 8

**Fig.8** Approximation of pitching moment due to heaving mode, $\mathbf{Q}_{21}$, of the rectangular cross section by MS RFA

**d) Streamlined girder**

A streamlined bridge cross-section is assumed to be a symmetric "airfoil". The flutter derivatives for this cross-section were obtained by analytical method (Sec. 2.2) for the same sets of reduced frequencies $\{K_n\}$ as for the flat box section (Sec. 5.1a). The results of the RFA by LS and MS formulations are shown in **Fig. 9**. The coefficients of the approximation function for MS formulation were found to be:

$$\mathbf{A}_0 = \begin{bmatrix} 1.3043 & 3.5334 \\ 0.3354 & 0.8738 \end{bmatrix}, \quad \mathbf{A}_1 = \begin{bmatrix} 3.3842 & 2.3576 \\ 0.7989 & -0.1875 \end{bmatrix},$$

$$\mathbf{D} = \begin{bmatrix} 3.4691 & 3.2670 \\ 0.8526 & 0.8641 \end{bmatrix}, \quad \mathbf{E} = \begin{bmatrix} -0.0145 & 0.0782 \\ -0.2304 & 0.2595 \end{bmatrix},$$

$$\lambda_1 = 0.1912, \quad \lambda_2 = 0.7477.$$

The results indicate that all the components of **Q** can be sufficiently approximated with only one lag term in the approximation functions. In that case the overall approximation error (30) is small, but the fit precision in the isolated points of $\{K_n\}$ may be poor. Addition of one more lag term guarantees high approximation precision for all the range of the reduced frequencies.

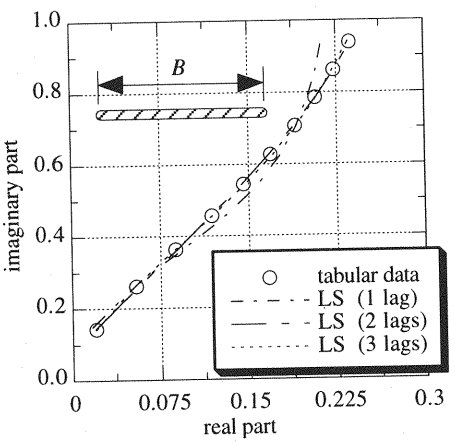


a) Least-squares RFA formulation

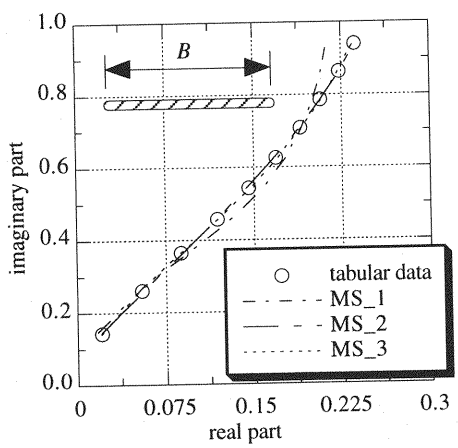


a) Minimum state RFA formulation

**Fig.9** Approximation of pitching moment due to heaving mode, $\mathbf{Q}_{21}$, of streamlined girder with different number of lag terms

### (2) Comparison of Least-Squares and Minimum-State RFA Formulations

The results of approximations show the similar fitting abilities of LS and MS RFA formulations due to different number of lag terms. However, the certain number of lag terms in both formulations does not result in the same number of newly introduced states (aerodynamic dimension). Recalling (22) and (27) the relationship between aerodynamic dimensions of LS and MS RFA is,

$$\underbrace{n_a = n \cdot n_l}_{\substack{\text{Aerodynamic} \\ \text{dimension of} \\ \text{LS RFA}}} > \underbrace{n_a = n_l}_{\substack{\text{Aerodynamic} \\ \text{dimension of} \\ \text{MS RFA}}} \qquad (33)$$

where $n$ is the number of degrees of freedom of the model and $n_l$ is the number of lag terms. Thus, the state-space realizations of MS RFA are significantly smaller than the realizations of LS RFA.

**Figure 10** compares the approximation of the flat box section of both RFA methods solely in terms of the total approximation errors $J$ (30) as a function of the aerodynamic dimension. Both methods show the significant fit improvement between one lag term and two lag terms, while the addition of third lag gives small improvement of the approximation precision. **Fig. 11**, which shows the total errors of approximations of the streamlined section, confirms the above findings. In this case the level of the errors is 3 times smaller than in case of the flat box section.

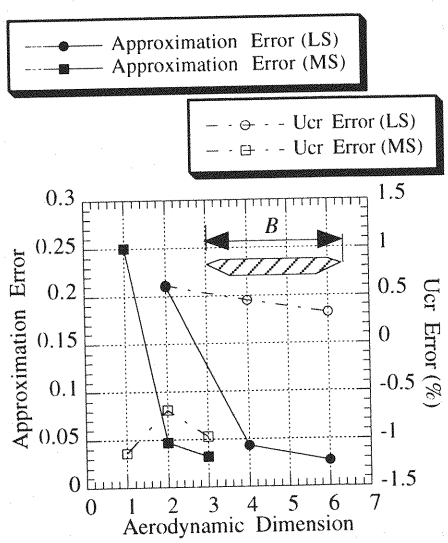


**Fig.10** Error of approximation and error of flutter wind speed for flat box cross section

**Figs. 10** and **11** show also the relative error of prediction of critical flutter wind speed with respect to the flutter wind velocity computed by conventional method (Sec 1.3). The computation of the critical wind speed, in case of state space realizations, is straightforward, since for fixed wind velocity the damping ratios and natural frequencies can be determined by the complex eigenvalue

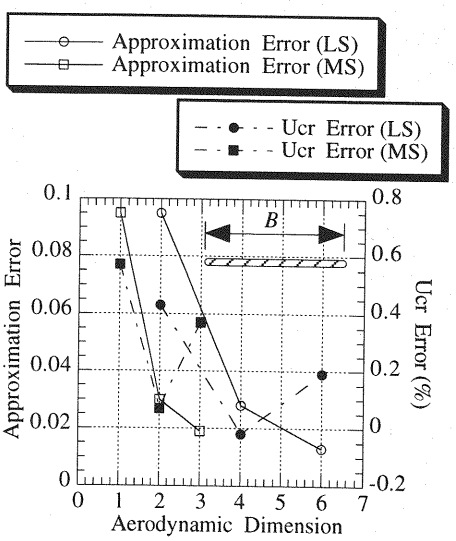


**Fig.11** Error of approximation and error of flutter wind speed for streamlined cross section

analysis. The increase of approximation functions by additional lag terms does not directly result in the improvement of flutter wind speed computation. It was found in this study that the prediction of flutter wind speed with application of RFA results in small error with respect to the conventional method. The prediction can be significantly improved by weighting the region close to the reduced frequency related to the flutter wind speed.

## 6. CONCLUSIONS

The rational function approximations of unsteady aerodynamic forces acting on the bridge deck provides the time domain description of the flutter problem. The resulting state space equation of motion simplifies bridge deck flutter prediction and makes design of vibration suppression systems simple and straightforward. Since the resulting equation of motion is in time domain, it also gives the possibility of analysis of aerodynamic problems with structural nonlinearities.

The proposed approximations can approximate unsteady aerodynamic forces with high approximation precision. The minimum-state RFA formulation provides only slightly larger approximation error than least-squares method with the significantly smaller aerodynamic dimension than LS RFA.

To maintain the accuracy, the number of added aerodynamic states is found to be 1 for streamlined section, 2 for flat box section and 3 for conventional truss section.

**ACKNOWLEDGMENT:** Data of unsteady aerodynamic forces used in this paper was provided by Honshu-Shikoku Bridge Authority and Prof. Matsumoto, M, Kyoto University. Their kind cooperation is gratefully acknowledged. This study is partially supported by Honshu-Shikoku Bridge Authority.

## REFERENCES

1) T. Theodorsen and I. Garrick: *Mechanism of Flutter, a Theoretical and Experimental Investigation of the Flutter Problem*, N.A.C.A. Report 689, 1940.
2) K. Roger: *Airplane Math Modeling Methods For Active Control Design*, AGARD-CP-288, 1977.
3) H. Dunn: *An Analytical Technique for Approximating Unsteady Aerodynamics in the Time Domain*, NASA TP-1738, 1980.
4) Karpel and Mordechay: *Design for Active and Passive Flutter Suppression and Gust Alleviation*, NASA CR-3482, 1981.
5) S. Tiffany and W. Adams: *Nonlinear Programming Extensions to Rational Function Approximation Methods for Unsteady Aerodynamic Forces*, NASA TP-2776, 1988.
6) R. Scanlan and J. Tomko: "Airfoil and Bridge Deck Flutter Derivatives", *J. Eng. Mech. Div.*, ASCE, 97, no. EM6, pp. 1717-1737, 1971.
7) Abel and Irving: *An Analytic Technique for Predicting the Characteristics of a Flexible Wing Equipped With an Active Flutter-Suppression System and Comparison With Wind-Tunnel Data*, NASA TP-1367, 1979.
8) J. Masukawa: "A Finite State Model for Unsteady Aerodynamic Forces of Various Bridge Decks", Master Thesis, University of Tokyo, 1994 (Japanese).
9) Y. Fujino and M. Iwamoto, et al: "Wind Tunnel Experiments Using U3 Models and Response Prediction for a Long-Span Suspension Bridges", *J. Wind Engineering and Industrial Aerodynamics*, vol. 41-44, pp. 1333-1344, 1992.
10) T. Miyata, H. Sato, R. Toriumi, M. Kitagawa and H. Katsuchi: "Full Model Wind Tunnel Study of the Akashi Kaikyo Bridge", *Proceedings of 9th International*

*Conference on Wind Engineering*, New Delhi, India, pp. 793-802, 1995.

11) M. Matsumoto, Y. Niihara and Y. Kobayashi: "On Mechanism of Flutter Phenomena for Structural Sections", *JSCE Journal of Structural Engineering*, vol. 40A, pp. 1019-1024, 1994 (Japanese).

**(Received October 2, 1995)**